



In vivo and in silico evaluation of a new nitric oxide donor, S,S' -dinitrosobucillamine

Marie-Lynda Bouressam, Benjamin Meyer, Ariane Boudier, Igor Clarot, Pierre Leroy, Alessandro Genoni, Manuel Ruiz-Lopez, Philippe Giummelly, Patrick Liminana, Valérie Salgues, et al.

► To cite this version:

Marie-Lynda Bouressam, Benjamin Meyer, Ariane Boudier, Igor Clarot, Pierre Leroy, et al.. In vivo and in silico evaluation of a new nitric oxide donor, S,S' -dinitrosobucillamine. Nitric Oxide: Biology and Chemistry, 2017, 71, pp.32-43. 10.1016/j.niox.2017.10.004 . hal-01665352

HAL Id: hal-01665352

<https://hal.univ-lorraine.fr/hal-01665352>

Submitted on 15 Dec 2017

HAL is a multi-disciplinary open access archive for the deposit and dissemination of scientific research documents, whether they are published or not. The documents may come from teaching and research institutions in France or abroad, or from public or private research centers.

L'archive ouverte pluridisciplinaire **HAL**, est destinée au dépôt et à la diffusion de documents scientifiques de niveau recherche, publiés ou non, émanant des établissements d'enseignement et de recherche français ou étrangers, des laboratoires publics ou privés.

***IN VIVO AND IN SILICO EVALUATION OF A NEW NITRIC OXIDE DONOR,
S,S'-DINITROSOBUCILLAMINE***

**Marie-Lynda BOURESSAM^a, Benjamin MEYER^{b,c}, Ariane BOUDIER^a, Igor
CLAROT^a, Pierre LEROY^a, Alessandro GENONI^{b,c}, Manuel RUIZ-LOPEZ^{b,c}, Philippe
GIUMMELLY^a, Patrick LIMINANA^a, Valérie SALGUES^a, Mostafa KOUACH^d,
Caroline PERRIN-SARRADO^a, Isabelle LARTAUD^a, François DUPUIS^a**

^a Université de Lorraine, CITHEFOR EA 3452, Faculty of Pharmacy, BP 80403, F-54000
Nancy Cedex, France

^b Université de Lorraine, SRSMC UMR 7565, Faculty of Sciences and Technologies, F-54500
Vandoeuvre-lès-Nancy, France

^c CNRS, SRSMC UMR 7565, Faculty of Sciences and Technologies, F-54500 Vandoeuvre-
lès-Nancy, France

^d Université de Lille 2, Plateau de Spectrométrie de Masse - GRITA EA 7365, Faculty of
Pharmacy, BP 83, F-59006 Lille, France

CORRESPONDING AUTHOR : François DUPUIS

CITHEFOR EA3452, Faculty of Pharmacy, 5 rue Albert Lebrun, BP 80403, F-54000 Nancy
Cedex, France

e-mail: Francois.Dupuis@univ-lorraine.fr

phone: +33 3 72 74 72 72

ABBREVIATIONS

BUC(NO)₂: S,S'-dinitrosobucillamine

BUC(SH)₂: bucillamine

GSNO: S-nitrosoglutathione

ISDN: isosorbide dinitrate

MAP: mean arterial pressure

NACNO: S-nitroso-N-acetylcysteine

PAP: pulse arterial pressure

RSNO(s): S-nitrosothiol(s)

SNAP: S-nitroso-N-acetylpenicillamine

SNOPCs: S-nitrosophytochelators

SNP: sodium nitroprusside

ABSTRACT

Purpose. In a previous work, we have synthesized a new dinitrosothiol, *i.e.* *S,S'*-dinitrosobucillamine BUC(NO)₂ combining *S*-nitroso-*N*-acetylpenicillamine (SNAP) and *S*-nitroso-*N*-acetylcysteine (NACNO) in its structure. When exposed to isolated aorta, we observed a 1.5-fold increase of [•]NO content and a more potent vasorelaxation (1 log higher pD₂) compared to NACNO and SNAP alone or combined (Dahboul *et al.*, 2014). In the present study, we analyzed the thermodynamics and kinetics for the release of [•]NO through computational modeling techniques and correlated it to plasma assays. Then BUC(NO)₂ was administered *in vivo* to rats, assuming it will induce higher and/or longer hypotensive effects than its two constitutive *S*-mononitrosothiols.

Methods. Free energies for the release of [•]NO entities have been computed at the density functional theory level assuming an implicit model for the aqueous environment. Degradation products of BUC(NO)₂ were evaluated *in vitro* under heating and oxidizing conditions using HPLC coupled with tandem mass spectrometry (MS/MS). Plasma from rats were spiked with RSNO and kinetics of RSNO degradation was measured using the classical Griess-Saville method. Blood pressure was measured in awake male Wistar rats using telemetry (n = 5, each as its own control, 48 h wash-out periods between subcutaneous injections under transient isoflurane anesthesia, random order: 7 mL/kg vehicle, 3.5, 7, 14 μmol/kg SNAP, NACNO, BUC(NO)₂ and an equimolar mixture of SNAP+NACNO in order to mimic the number of [•]NO contained in BUC(NO)₂). Variations of mean (ΔMAP, reflecting arterial dilation) and pulse arterial pressures (ΔPAP, indirectly reflecting venodilation, used to determine effect duration) *vs.* baseline were recorded for 4 h.

Results. Computational modeling highlights the fact that the release of the first [•]NO radical in BUC(NO)₂ requires a free energy which is intermediate between the values obtained for SNAP and NACNO. However, the release of the second [•]NO radical is significantly favored by the concerted formation of an intramolecular disulfide bond. The corresponding oxidized compound was also characterized as related substance obtained under degradation conditions. The *in vitro* degradation rate of BUC(NO)₂ was significantly greater than for the other RSNO. For equivalent low and medium [•]NO-load, BUC(NO)₂ produced a hypotension identical to NACNO, SNAP and the equimolar mixture of SNAP+NACNO, but its effect was greater at higher doses (-62±8 and -47±14 mmHg, maximum ΔMAP for BUC(NO)₂ and SNAP+NACNO, respectively). Its duration of effect on PAP (-50%) lasted from 35 to 95 min, *i.e.* shorter than for the other RSNO (from 90 to 135 min for the mixture SNAP+NACNO).

56 **Conclusion.** A faster metabolism explains the abilities of BUC(NO)₂ to release higher
57 amounts of [•]NO and to induce larger hypotension but shorter-lasting effects than those
58 induced by the SNAP + NACNO mixture, despite an equivalent [•]NO-load.

59 **Key-words**

60 *S,S'*-dinitrosobucillamine; telemetry; awake rat; mean arterial pressure; pulse arterial pressure;
61 *ab initio* calculations

1. INTRODUCTION

Decrease of nitric oxide (NO) bioavailability is associated with cardiovascular diseases such as hypertension, atherosclerosis, angina pectoris [1]. Currently available NO donors induce tolerance and oxidative stress [2; 3]. *S*-nitrosothiols (RSNO) are interesting candidates for delivering NO [4] as they do not induce such side effects [5]. They have a longer half-life [6], induce vasorelaxation [7], prevent platelet aggregation [8] and are currently thought to play a major role in the endogenous storage and transport of NO [9; 10]. *S*-nitrosothiols have also the advantage of releasing both NO and thiols which exhibit antioxidant and anti-inflammatory properties.

The rate and/or quantity of released NO vary according to the thiol carrying the SNO moiety. Therefore, numerous molecules exhibiting thiol functions are under consideration to define the best RSNO candidate. An interesting strategy relies on increasing NO -payload by synthesizing di- or poly-nitrosothiols. Such compounds may increase the amount of released NO , while limiting the drug quantity [11; 12] compared to most of the mononitrosothiols previously synthesized [9; 13]. Besides the NO -payload, Heikal *et al.* evaluated the bioactivity of a new RSNO subgroup: *S*-nitrosophytochelatin (SNOPCs). These oligopeptides expressed in plants are analogues of *S*-nitrosogluthathione (GSNO, an endogenous RSNO present in humans). Heikal *et al.* compared several SNOPCs, carrying 2 to 6 SNO moieties, with GSNO. When administered at equal molar concentrations of SNO, SNOPCs induce a more intense decrease of blood pressure than GSNO [14], even though their *in vitro* vasodilatory effect was equivalent to GSNO (again at equimolar concentrations of SNO) [12]. These results demonstrate that the molecule carrying the SNO moieties is also a major determinant of the biological activities of RSNO.

We previously synthesized a new RSNO, *S,S'*-dinitrosobucillamine ($\text{BUC}(\text{NO})_2$), which combines in its structure two mononitrosothiols: *S*-nitroso-*N*-acetylpenicillamine (SNAP) and *S*-nitroso-*N*-acetylcysteine (NACNO) [11]. The synthesis was performed using bucillamine ($\text{BUC}(\text{SH})_2$) which is a commercially available drug used to treat rheumatoid arthritis, in relation with its anti-inflammatory and antioxidant properties [15; 16]. In an aortic ring model, $\text{BUC}(\text{NO})_2$ induced vasorelaxation at lower concentrations (pD_2 7.8 ± 0.1 , with $\text{pD}_2 = -\log \text{EC}_{50}$, *i.e.* the molar concentration producing 50% of the maximal effect) than NACNO (6.4 ± 0.2), SNAP (6.7 ± 0.1) and the mixture of SNAP+NACNO (6.7 ± 0.2). Furthermore, the *in vitro* NO release was significantly higher from $\text{BUC}(\text{NO})_2$ (6-fold increase *versus* basal value) than from the SNAP+NACNO mixture (4-fold increase *versus* basal value) [11]. Altogether, these data suggest that $\text{BUC}(\text{NO})_2$ might be an interesting

candidate for the cardiovascular pathologies. However, those previous experiments did not evaluate the systemic effects.

Therefore, the present work was conducted to further characterize BUC(NO)₂. In this aim, we used molecular modeling to study the thermodynamics of the two [•]NO entities released from BUC(NO)₂ and the resulting bucillamine derived product. We also monitored *in vitro* the obtained degradation products by using HPLC-MS/MS, and examined *in vitro* in plasma from Wistar rat spiked with RSNO the rate of decomposition of BUC(NO)₂ as compared to SNAP, NACNO and SNAP+NACNO. Then, we explored the systemic effects and duration of action of BUC(NO)₂ *in vivo*, using awake male Wistar rats equipped with telemetric devices. On the basis of its [•]NO-release profile, we assume that BUC(NO)₂ would induce higher and/or longer *in vivo* hypotensive effects than its constitutive *S*-mono-nitrosothiols SNAP, NACNO. We also compare to an equimolar mixture of NACNO plus SNAP (in order to mimic the quantity of [•]NO contained in the BUC(NO)₂ solutions). The intensity of hypotension was evaluated on the basis of changes in mean arterial pressure (MAP) which reflect the *in vivo* dilating effect of RSNO on arteries and arterioles. Changes in pulse arterial pressure (PAP) were used to determine the duration of effect, as we previously showed, using similar protocols, that PAP allows a precise evaluation of RSNO effects duration [17; 18].

2. MATERIAL and METHODS

2.1. Reagents and standards

All reagents were of analytical grade and used without further purification. *N*-(2-mercapto-2-methylpropanoyl)-*L*-cysteine (BUC(SH)₂) was purchased from Discovery Fine Chemicals (Wimborne Dorset, United Kingdom). *N*-acetylpenicillamine (NAP), *N*-acetylcysteine (NAC) and all other reagents were from Sigma-Aldrich (Saint Quentin Fallavier, France). Ultrapure deionized water (> 18.2 MΩ.cm) was used to prepare all solutions. Phosphate-buffered saline (PBS) was prepared as follows: [Na₂HPO₄] = 6.48 × 10⁻³M, [KH₂PO₄] = 1.47 × 10⁻³M, [NaCl] = 137.93 × 10⁻³M, and [KCl] = 2.68 × 10⁻³M, final pH was adjusted to 7.4 with NaOH (40%). All the RSNO were extemporaneously synthesized at a final concentration of 10⁻² M, by reacting *N*-acetylpenicillamine, *N*-acetylcysteine or BUC(SH)₂ with NaNO₂ in acidic medium, as previously described [11; 17; 19]. Solutions were adjusted to pH 7.4 by adding NaOH 40% then two-fold diluted in 10⁻² M phosphate buffer pH 7.4.

Final solutions showed high osmolarity (1.8 osm/L). The volumes and dilutions required to reach isotonic solutions for injection were too important. Therefore, hyperosmolar solutions were used. Animals received the same volume for each injection (solutions have been diluted according to the expected dose in a final volume of 3.4 mL). In the control (vehicle) solution, nitrite ions were replaced by a 0.2 M NaCl solution.

Due to their light- and temperature-sensitivity, final solutions were stored in the dark at 4°C, no longer than 5 days for NACNO and SNAP, and 10 h for BUC(NO)₂, according to their stability previously described by Dahboul *et al.* [11].

2.2. Theoretical chemistry calculations

The computational approach was chosen according to our previous investigations [20]. Specifically, we performed Density Functional Theory calculations (B3PW91 functional [21] with the 6-311+G(d,p) basis-set). In order to account for the influence of the physiological medium, we assumed an ionized system (anionic form of the carboxylic group) surrounded by an aqueous environment (described by an implicit solvation model [22]). A thorough analysis of BUC(NO)₂ conformations was first performed. In the most stable structure, the peptide bond is (as expected) in *trans* conformation and both RS-NO bonds adopt an *anti* conformation. From this structure, we calculated the sequential homolytic bond dissociation free energies (at 298.15 K) for the two RS-NO bonds. The two possible monoradical and the biradical species were studied. Besides, we considered a hypothetical mechanism for the second *NO dissociation in which the formation of an incipient disulfide bond significantly stabilizes the process. All computations were carried out using the Gaussian09 package [23].

2.3. Identification of degradation product(s) from *S,S'*-dinitrosobucillamine

In order to check the reliability of the theoretical predictions, we have carried out LC-MS/MS experiments aimed at identifying the molecular structure of a main degradation product obtained after exposure of BUC(NO)₂ to either heating (55°C, 120 min) or H₂O₂ (10.0% v/v, 15 min). Such conditions have been previously used in the field of toxicology predictions [24].

The stock BUC(NO)₂ solution (10⁻² M in phosphate buffer pH 7.4) with and without H₂O₂ was diluted one thousand times in the mobile phase before injection in the LC system.

LC-MS/MS experiments were carried out on a UFLC-XR device (Shimadzu) coupled to a QTRAP® 5500 MS/MS hybrid system triple quadrupole/linear ion trap mass spectrometer (AB Sciex, Foster City, USA) equipped with a turbo VTM ion source. Instrument control, data acquisition and processing were performed using Analyst 1.5.2 software. The RP-LC separation was carried out at 40°C on a Nucleosil C18 100 AB (5 µm

250 x 4 mm) column (Macherey Nagel) at a flow rate of 0.8 mL/min and with an isocratic mobile phase CH₃CN-H₂O-HCOOH (30/69.9/0.1, v/v/v). The injection volume was 10 µL. MS analysis was carried out in negative ionization mode using an ion spray voltage of -4500V. The curtain gas flow was set at 25 psi using nitrogen. The turbo VTM ion source was set at 550°C. Nebulizer gas and auxiliary gas flow (air) were set at 50 psi. Acquisition was performed in IDA “Information Dependent Acquisition” method. The IDA method consists of a switch between MS (survey scan) and MS/MS (dependent scan) in a single run.

2.4. *In vitro* measurement of *S,S'*-dinitrosobucillamine degradation in spiked plasma

In order to confirm our *in silico* and *in vitro* findings, we compared the rate of degradation of BUC(NO)₂ *in vitro* to those of SNAP, NACNO and SNAP+NACNO. Briefly, rats were anesthetized with isoflurane, heparinized (500 UI) and blood was collected on heparinized tubes directly from the abdominal aorta. Blood was then centrifuged (2000g, 15 min, 4°C), plasma collected and immediately spiked with either BUC(NO)₂, SNAP, NACNO or SNAP+NACNO (RSNO/plasma volume ratio of 1/10). Plasma samples were then stored under agitation at 37°C.

The loading doses were chosen to achieve a plasma concentration of 175.0 µmol/L for SNAP and NACNO and 87.5 µmol/L for SNAP+NACNO and BUC(NO)₂ (*i.e.* an equivalent *NO-load of 175.0 µmol/L). These concentrations are equivalent to the theoretical maximal concentrations following *in vivo* administration (7.0 µmol/kg for SNAP and NACNO and 3.5 µmol/kg for SNAP+NACNO and BUC(NO)₂, considering a total blood volume of 40 mL/kg).

The RSNO were quantified at 0, 5 and 15 min after RSNO load (based on the kinetics of the *in vivo* blood pressure effect) by the Griess-Saville assay [25]. Briefly, the samples were diluted in 0.4 M acetoacetic buffer (pH = 2.5) in duplicates (two dilutions tested, 1/20 and 1/50, final volume of 200 µL) and then incubated with 40 µL of a 0.6% (w/v) sulfanilamide solution supplemented with 0.2% (w/v) of HgCl₂. The diazonium salt so formed was reacted with 10 µL of a 0.6% (w/v) *N*-(1-naphthyl) ethylenediamine solution to form a chromophoric azo product that absorbs at 540 nm. For each drug, the calibration curve was made with the corresponding RSNO in phosphate buffer. Free nitrite ions (quantified by Griess assay) as well as RSNO in non-fortified plasma were below the limit of detection (< 1 µmol/L) and could thus be neglected as regards to the RSNO load. Results are presented as a percentage of the initial quantity of RSNO added to the plasma.

2.5. Animals, telemetry and hemodynamics measurement

All experiments were performed in accordance with the European Community guidelines (2010/63/EU) for the use of experimental animals. The protocols and procedures

were approved by an advisory regional ethical committee on animal experiments (project “BucNOtelem”, APAFIS#2119-2015100214406732 v3).

Surgery was performed on 4 month-old male normotensive outbred Wistar rats (Rj/Han: Wi, Janvier, France) ($n = 5$) and the experiments conducted between 5 and 10 months of age. Animals had mild restriction to standard rat chow (A04, Safe, France, 25 g per day) in order to maintain their body weight around 500 g until the end of experiments. They drank water (Aqua-clear®, Culligan, USA) *ad libitum*. Rats were equipped with telemetric devices (PA-C40, Data Sciences International, USA; abdominal aorta) under isoflurane anesthesia and aseptic surgery (48 h analgesia with paracetamol 60 mg/kg/day *per os*, then 1 month recovery). Each rat was used as its own control. All the injections were performed between 11 and 12 a.m., subcutaneously (21-G needle) under transient (less than 5 min) isoflurane anesthesia in order to standardize injections [18] and to reduce stress. Each rat received control solution, then, in a random order with 2-day wash-out period and at distinct injection sites, SNAP, NACNO, BUC(NO)₂ or the mixture SNAP+NACNO at 3.5, 7, and 14 $\mu\text{mol/kg}$. At the end of the experiments, the effects of the RSNO were compared to that other of •NO-donors, *i.e.* isosorbide dinitrate (ISDN, 21, 42 and 85 $\mu\text{mol/kg}$) and sodium nitroprusside (SNP, from 0.0035 up to 3.5 $\mu\text{mol/kg}$). Animals were then euthanized (pentobarbitone 120 mg/kg).

Hemodynamics were recorded in awake rats (Ponemah 5.1 software, Data Sciences International, USA, 250 Hz sampling rate). Basal MAP (area under the pressure wave for each valid cardiac cycle), PAP (difference between the maximum and minimum pressure values of each pressure wave) and heart rate (HR) were recorded during minimum 2 h and averaged on the last 5 min to obtain baseline values. For each RSNO dose, MAP, PAP and HR were recorded continuously for 4 h following injection and their variations *vs.* baseline values were averaged on 1 min every 5 min.

As mentioned above, changes in MAP were analyzed as RSNO are known to induce arterial and arteriolar dilatation. Changes in PAP were analyzed as RSNO are known to induce large venodilation [26]; we previously published a similar approach in [17; 18]. As PAP cannot physiologically fall under 15 mmHg, this parameter is more suitable to accurately determine the effect duration.

2.6. Statistical analysis

Results are expressed as means \pm S.E.M.

Significant differences in *in vitro* RSNO degradation were determined by a two-way ANOVA (variables: “time” and “drug”) followed by a *post-hoc* Bonferroni test.

Significant differences in MAP, PAP and HR variations between controls, SNAP, NACNO, SNAP+NACNO or BUC(NO)₂ were determined at equivalent [•]NO-load (half dose for SNAP+NACNO and BUC(NO)₂ *versus* mononitrosothiols) by a two-way ANOVA (variables: “time” and “drug”) for repeated measurements (time factor) followed by a *post-hoc* Bonferroni test.

The duration of effects on PAP, MAP and HR variations was evaluated individually as the time of the last value remaining significantly lower (PAP and MAP) or higher (HR) than the mean of the next 20 points. These durations and the maximal hypotension values were then compared between groups by a two-way ANOVA (variables “dose” and “drug”) followed by a *post-hoc* Bonferroni test.

The null hypothesis was rejected at $p < 0.05$. Statistical analyzes were performed using GraphPad Prism version 5 (GraphPad Software).

3. RESULTS

3.1. Thermodynamics of [•]NO release from *S,S'*-dinitrosobucillamine: computational study

Since there are two different SNO groups in BUC(NO)₂, one can imagine two different pathways, depending on which S-NO bond dissociates first. In the first pathway (P₁), the primary SNO (*i.e.* the one attached to the RCH₂ group) dissociates first, and the sequential [•]NO dissociation free energies, which are necessary to form the monoradical and the diradical species, amount 16.4 and 16.9 kcal.mol⁻¹, respectively. In the second pathway (P₂), the tertiary SNO (*i.e.* the one attached to the RC(CH₃)₂ group) dissociates first, and the corresponding energies are 16.0 and 16.6 kcal.mol⁻¹.

The second dissociation process is much faster than the first one because of the concerted formation of a disulfide bond, which substantially stabilizes the system. Accordingly, the second dissociation proceeds through a transition structure that leads to a disulfide product (Figure 1) and it is only 9.1 kcal.mol⁻¹ above the monoradical species in path P₁ (or 12.3 kcal.mol⁻¹ in P₂). As a consequence of this low activation free energy for the second dissociation process, in BUC(NO)₂ the first dissociation step can be considered the rate determining for the double dissociation.

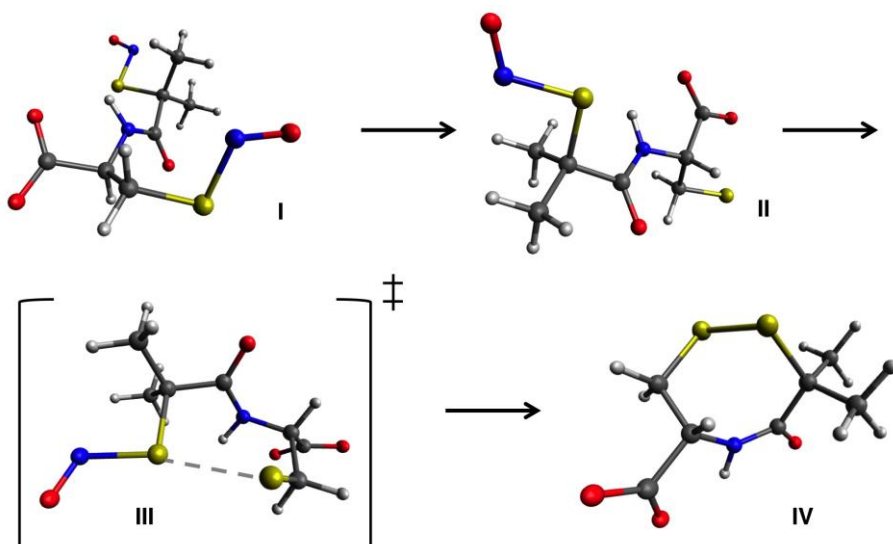


Figure 1. Calculated minimum energy structures for the double dissociation process of BUC(NO)₂ (I) along pathway P₁.

After the first (barrierless) [•]NO dissociation process leading to the monoradical (II), the system evolves through a transition structure (III) to form a disulfide-bond product (IV).

Applying transition state theory, and assuming first-order rate laws, the following kinetic constants have been roughly obtained from the quantum chemical models of BUC(NO)₂ (present work), SNAP and NACNO [20]:



3.2. Identification of the main degradation product of *S,S'*-dinitrosobucillamine

The degradation processes, monitored by mass-coupled liquid chromatography, led to similar results for both stress conditions. A chromatogram of a fresh BUC(NO)₂ solution is illustrated on Figure 2A with its MS/MS spectrum in Figure 2B showing a specific molecular ion at *m/z* 280. All the molecular structures determined in this part are described in Table 1.

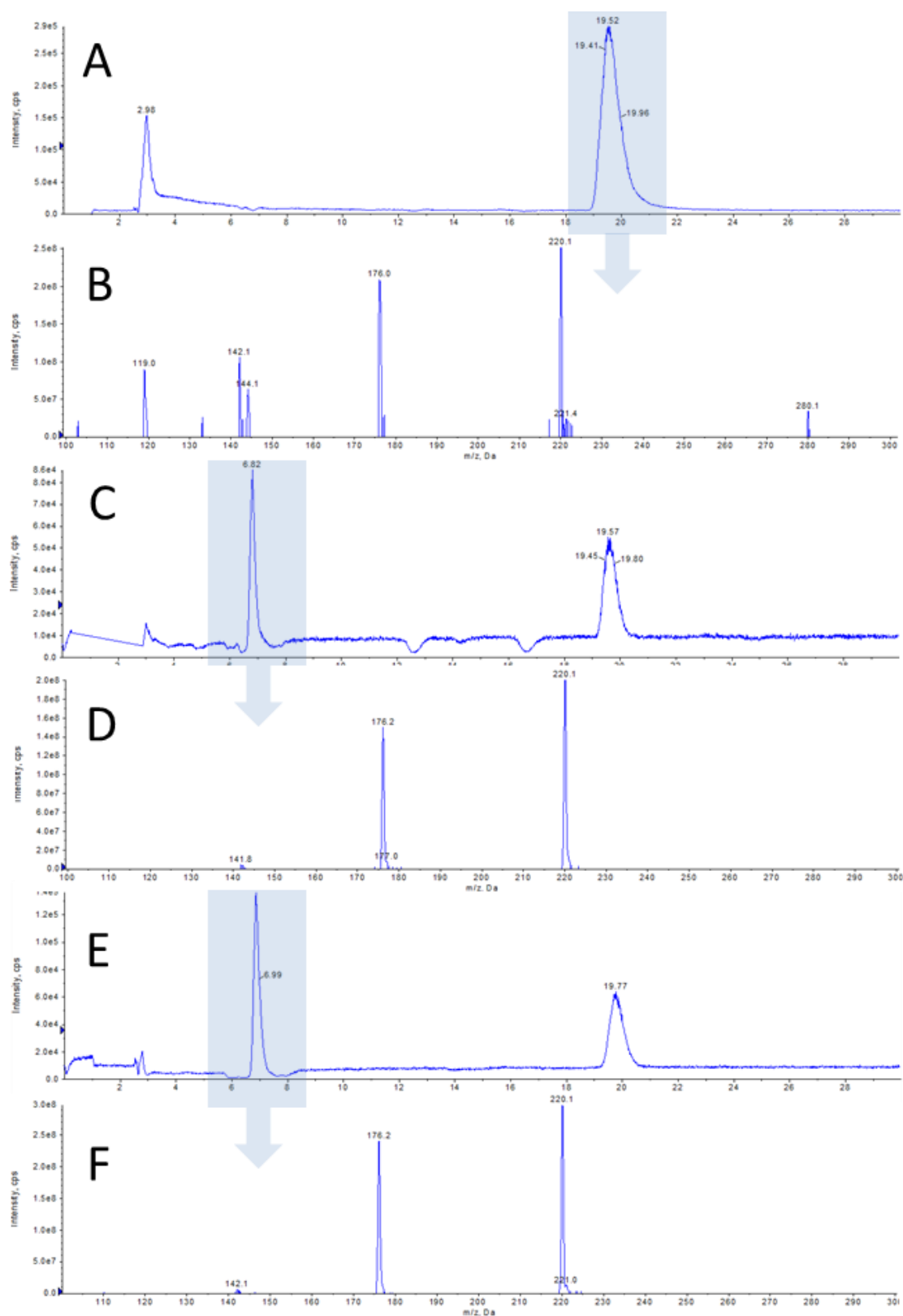


Figure 2. MS (survey scan) chromatograms and corresponding MS/MS spectra of the grey peak obtained for the degradation study.
 Panels A and B: fresh solution; panels C and D: after 15 min with H₂O₂; panels E and F: after 120 min at 55°C.

Table 1: Mass/charge (m/z) values and structures of the molecular ions found in the MS/MS spectra during the *in vitro* degradation study.

m/z (amu)	Ions	Structures [X] ⁻
280	M ₁	BUC(S-NO,S-NO)-H
220	M ₂	BUC(S-S)-H
176	M ₃	M ₂ -CO ₂
144	M ₄	M ₃ -S
142	M ₅	M ₃ -SH ₂

Degradation conditions presently used led to the appearance of a chromatographic peak at a retention time of 6.8 min. (Figure 2C and 2E for oxidation and heating, respectively). The MS/MS spectra of this degradation product are given in Figure 2D and 2F with a m/z major ion at 220 amu corresponding to the [BUC(S-S)-H]⁻ structure. It is important to note that no other molecular ions were detected at m/z values upper than m/z 300, leading to the conclusion that the disulfide bond formation is only favored through an intramolecular pathway. Furthermore, the mononitrosated bucillamine was not observed whatever the chromatogram under study, indicating that the denitrosation process is rapid and simultaneously concerns the two thiol groups included in the BUC(NO)₂ structure.

3.3.Kinetics for RSNO decomposition in plasma

We added RSNO to plasma *in vitro*, to evaluate their decomposition rate. As shown in Figure 3, a marked difference appears between BUC(NO)₂ and the other RSNO. At each time point (0, 5 and 15 min), the *in vitro* degradation of BUC(NO)₂ was significantly greater than that of SNAP, NACNO or SNAP+NACNO, indicating a faster metabolism and confirming our *in silico* and *in vitro* findings.

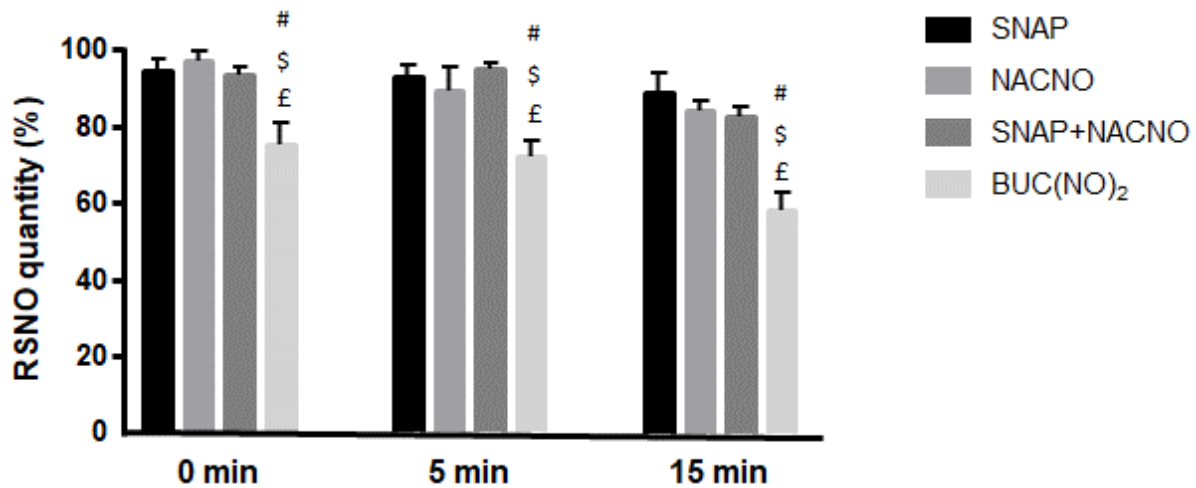


Figure 3. *In vitro* degradation rate of *S*-nitroso-*N*-acetylpenicillamine (SNAP), *S*-nitroso-*N*-acetylcysteine (NACNO), SNAP+NACNO and *S,S'*-dinitrosobucillamine (BUC(NO)₂). Each RSNO was added (to obtain a theoretical [•]NO concentration of 175 μmol/L) to freshly obtained plasma and quantified using the Griess-Saville assay (n= 9 to 14 per RSNO). Results are presented as percentage of the RSNO load (mean±SEM). $p_{\text{interaction}} = 0.0513$, p_{drug} and $p_{\text{time}} < 10^{-4}$; #: $p < 0.05$ vs SNAP; \$: $p < 0.05$ vs NACNO; £: $p < 0.05$ vs SNAP+NACNO (two-way ANOVA; *post-hoc* Bonferroni test).

3.4. Haemodynamic responses to RSNO

As previously observed when similar protocols are applied [17; 18], rats treated with the vehicle solution (controls) showed moderate increases in MAP (less than 20% vs. baseline, Figures 4 to 6) and HR (Figure 7) during the first 30 min after administration, related to the increase in activity during waking-up after the transient anesthesia. No significant change in PAP could be observed in controls (Figures 4 to 6).

The increases in MAP were masked when rats received RSNO, except for the lowest dose of BUC(NO)₂ (Figures 4 to 6). Each drug induced a dose-dependent hypotension (fall in MAP). When comparing the maximal hypotension produced by the different treatments, at doses that are expected to release similar amounts of [•]NO, there was no significant difference between BUC(NO)₂ and the SNAP+NACNO mixture at 3.5 and 7 μmol/kg, but a trend for a greater hypotension with BUC(NO)₂ compared to SNAP+NACNO at 14 μmol/kg (Table 2). The changes in MAP lasted from 5 (lowest doses) to 50 min (highest doses) with no significant differences amongst the treatments ($p_{\text{interaction}} = 0.0680$; $p_{\text{drug}} = 0.2418$; $p_{\text{dose}} < 10^{-4}$; data not shown).

These changes in MAP induced significant increases in HR (stimulation of the baroreflex) when compared to vehicle-treated animals (Figure 7). No noticeable difference

322 could be observed among the groups receiving RSNO. The duration of the changes in HR did
323 not differ amongst treatments, except for BUC(NO)₂ which induced a shorter effect than the
324 SNAP+NACNO mixture (Figure 8).

325 The duration of falls in PAP (around -15 mmHg for all drugs, whatever the doses used,
326 Figures 4 and 5) was dose-dependent. The effect of BUC(NO)₂ on PAP (from 37 to 96 min)
327 was significantly shorter than those of the other treatments (SNAP: 69 to 113 min; NACNO:
328 78 to 117 min) and the SNAP+NACNO mixture had the most prolonged impact on PAP (92
329 to 136 min, Figure 8).

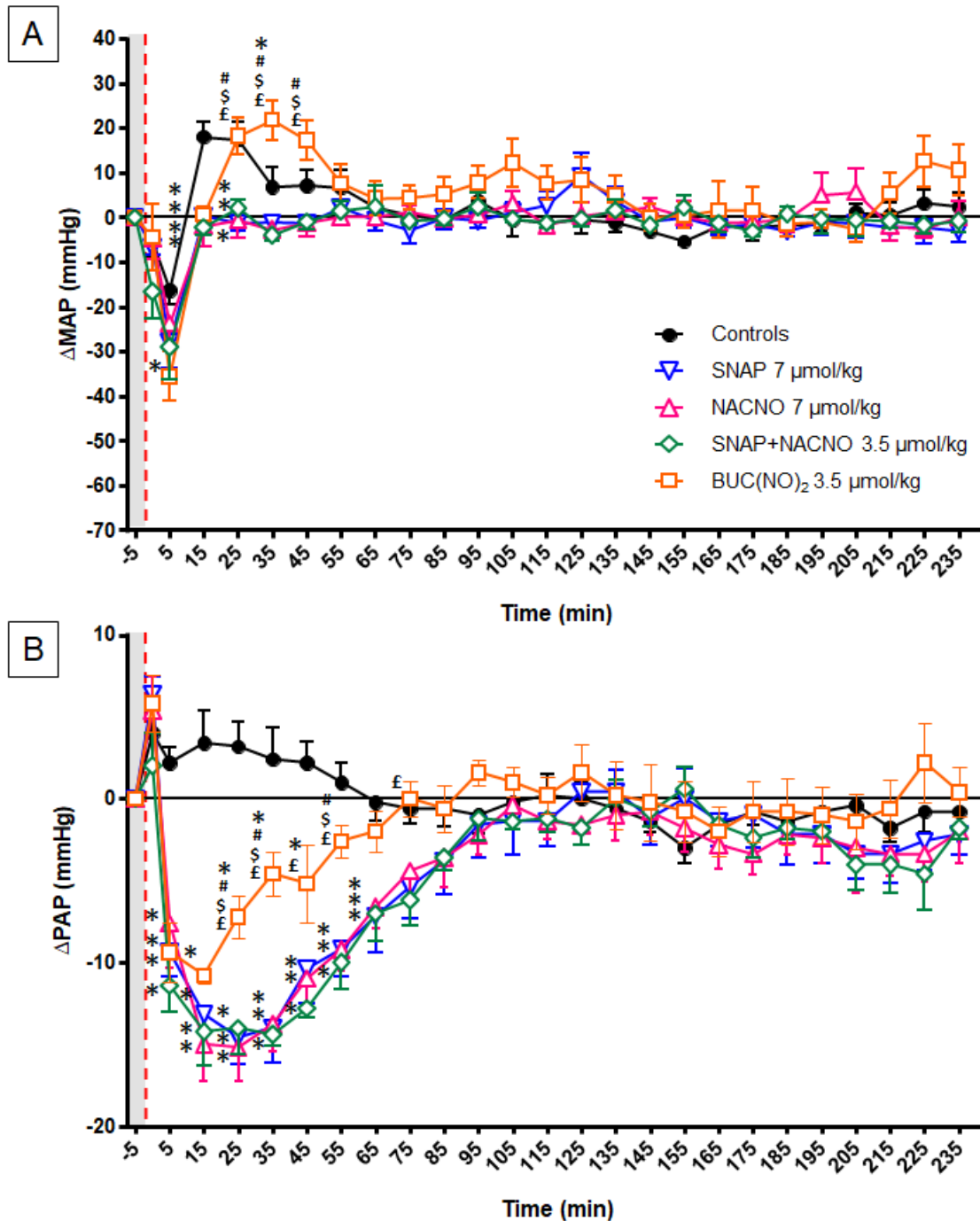


Figure 4. Impact of low doses of *S*-nitroso-*N*-acetylpenicillamine (SNAP), *S*-nitroso-*N*-acetylcysteine (NACNO), the mixture SNAP+NACNO and *S,S'*-dinitrosobucillamine (BUC(NO)₂) on mean arterial pressure (MAP, panel A) and pulse arterial pressure (PAP, panel B) variations (Δ) versus baseline.

For a better clarity, only one out of two values was plotted on the graph. Doses were compared on the basis of an equivalent 'NO-load (half dose for SNAP+NACNO and BUC(NO)₂ versus mononitrosothiols). Each animal (n = 5) received all the drugs, each dose of each drug separated a by 2-day wash-out period. Grey boxes represent the duration of anesthesia and the red vertical dashed line the time of injection. *: p < 0,05 vs controls; #: p < 0,05 vs SNAP; \$: p < 0,05 vs NACNO; £: p < 0,05 vs SNAP+NACNO; Panel A: p_{interaction} < 10⁻⁴; p_{drug} = 0.0688; p_{time} < 10⁻⁴; Panel B: p_{interaction} < 10⁻⁴; p_{drug} = 0.0210; p_{time} < 10⁻⁴; (two-way ANOVA; *post-hoc* Bonferroni test).

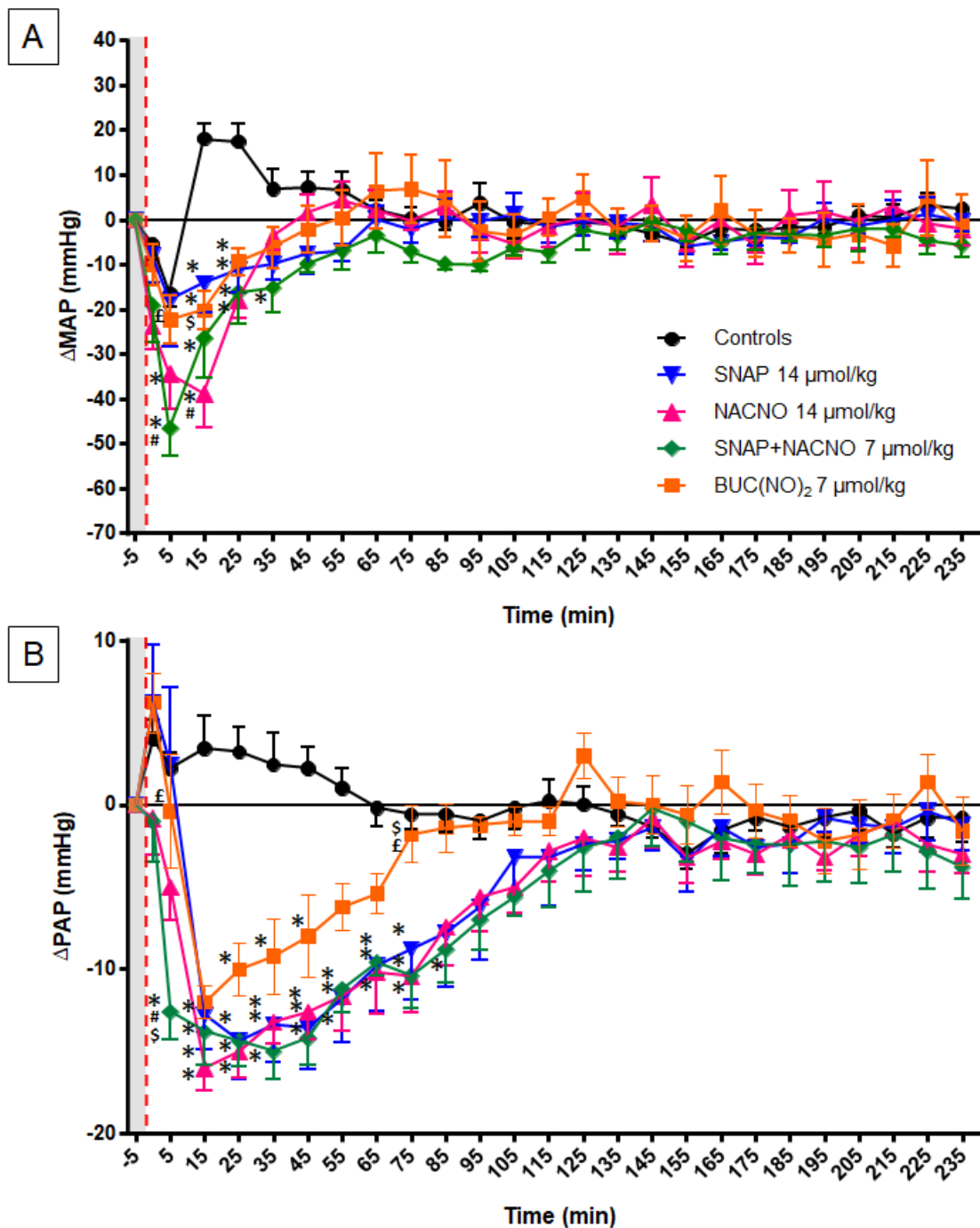


Figure 5. Impact of medium doses of *S*-nitroso-*N*-acetylpenicillamine (SNAP), *S*-nitroso-*N*-acetylcysteine (NACNO), the mixture SNAP+NACNO and *S,S'*-dinitrosobucillamine (BUC(NO)₂) on mean arterial pressure (MAP, panel A) and pulse arterial pressure (PAP, panel B) variations (Δ) versus baseline.

For a better clarity, only one out of two values was plotted on the graph. Doses were compared on the basis of an equivalent 'NO-load (half dose for SNAP+NACNO and BUC(NO)₂ versus mononitrosothiols). Each animal (n = 5) received all the drugs, each dose of each drug separated a by 2-day wash-out period. Grey boxes represent the duration of anesthesia and the red vertical dashed line the time of injection. *: p < 0,05 vs controls; #: p < 0,05 vs SNAP; \$: p < 0,05 vs NACNO; £: p < 0,05 vs SNAP+NACNO; Panel A: p_{interaction} < 10⁻⁴; p_{drug} = 0.2498; p_{time} < 10⁻⁴; Panel B: p_{interaction} < 10⁻⁴; p_{drug} = 0.0421; p_{time} < 10⁻⁴; (two-way ANOVA; *post-hoc* Bonferroni test).

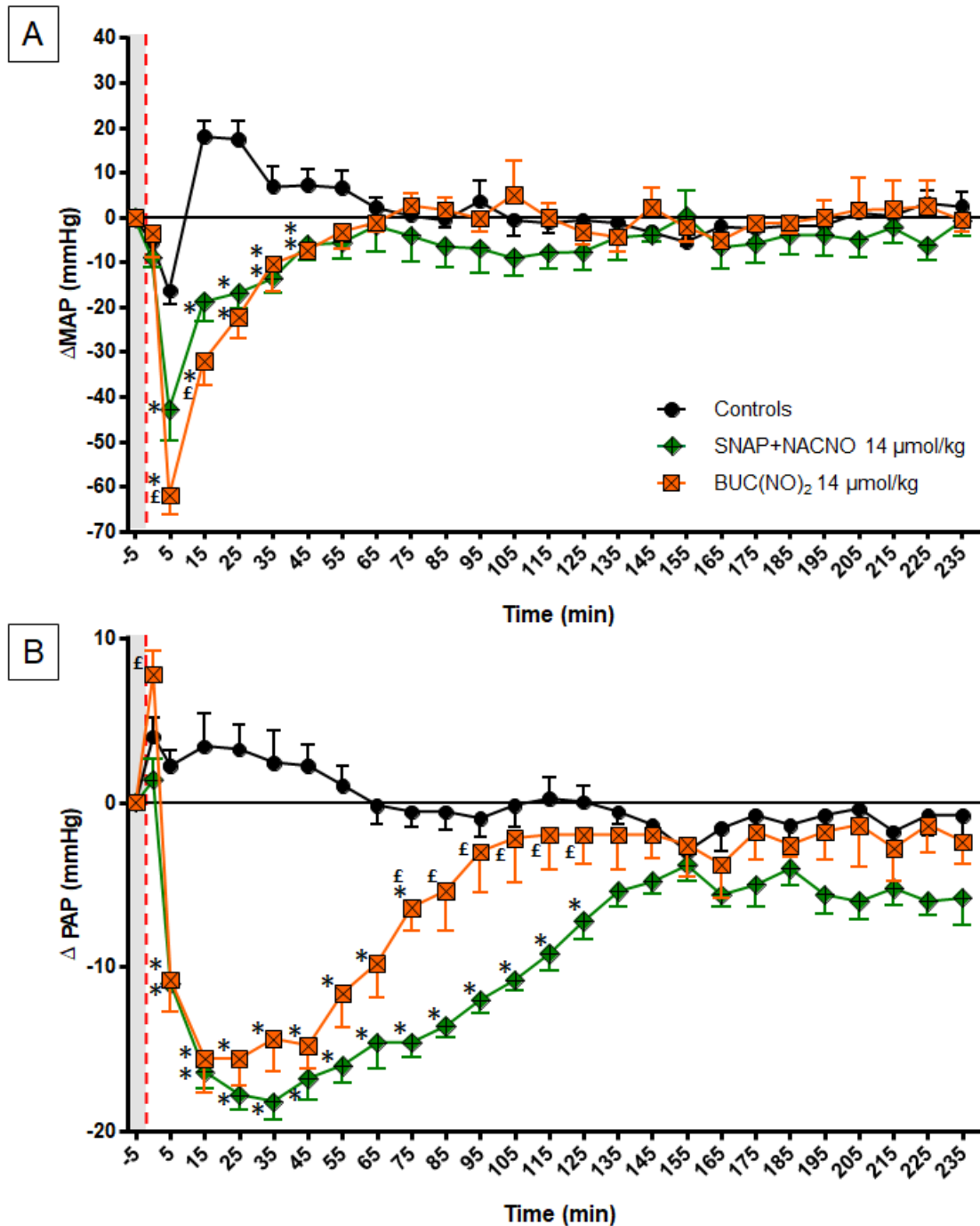


Figure 6. Impact of high doses of the mixture *S*-nitroso-*N*-acetylpenicillamine + *S*-nitroso-*N*-acetylcysteine (SNAP+NACNO) and *S,S'*-dinitrosobucillamine (BUC(NO)₂) on mean arterial pressure (MAP, panel A) and pulse arterial pressure (PAP, panel B) variations (Δ) versus baseline.

For a better clarity, only one out of two values was plotted on the graph. Each animal ($n = 5$) received all the drugs, each dose of each drug separated a by 2-day wash-out period. Grey boxes represent the duration of anesthesia and the red vertical dashed line the time of injection. *: $p < 0,05$ vs controls; £: $p < 0,05$ vs SNAP+NACNO; Panel A: $p_{\text{interaction}} < 10^{-4}$; $p_{\text{drug}} = 0.0979$; $p_{\text{time}} < 10^{-4}$; Panel B: $p_{\text{interaction}} < 10^{-4}$; $p_{\text{drug}} = 0.0003$; $p_{\text{time}} < 10^{-4}$; (two-way ANOVA; *post-hoc* Bonferroni test).

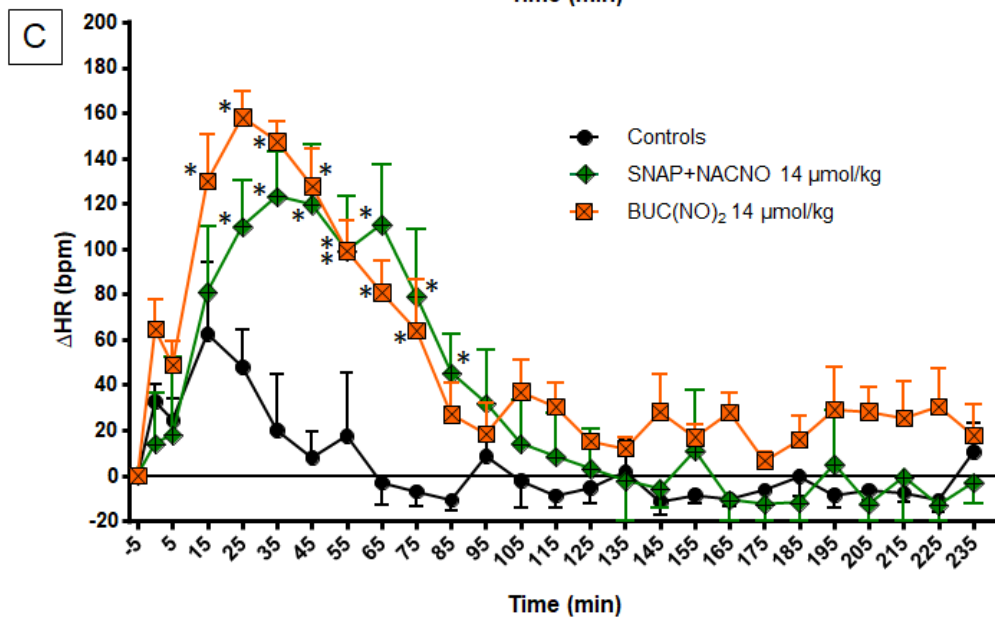
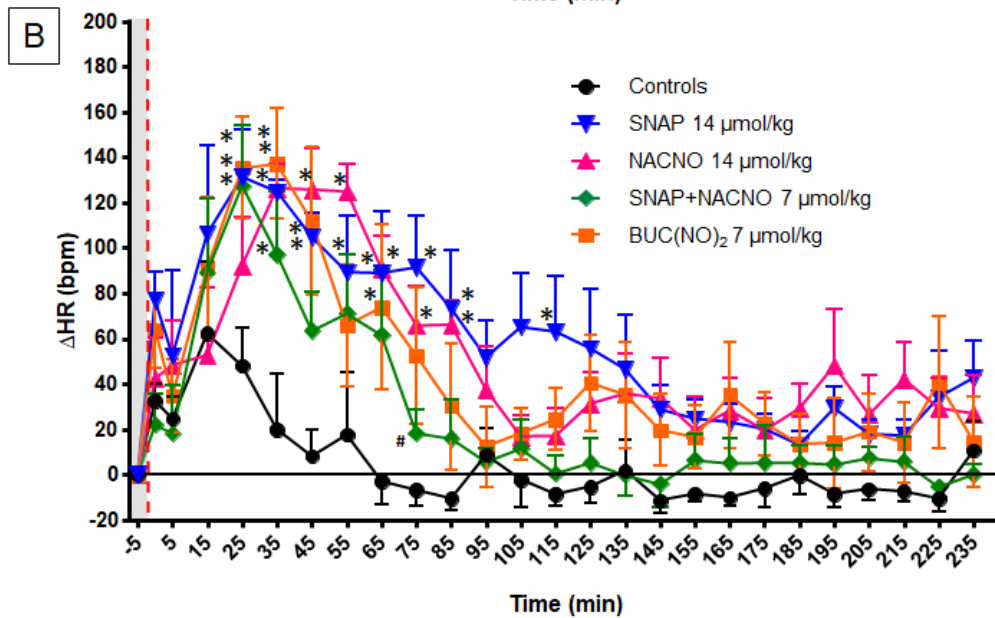
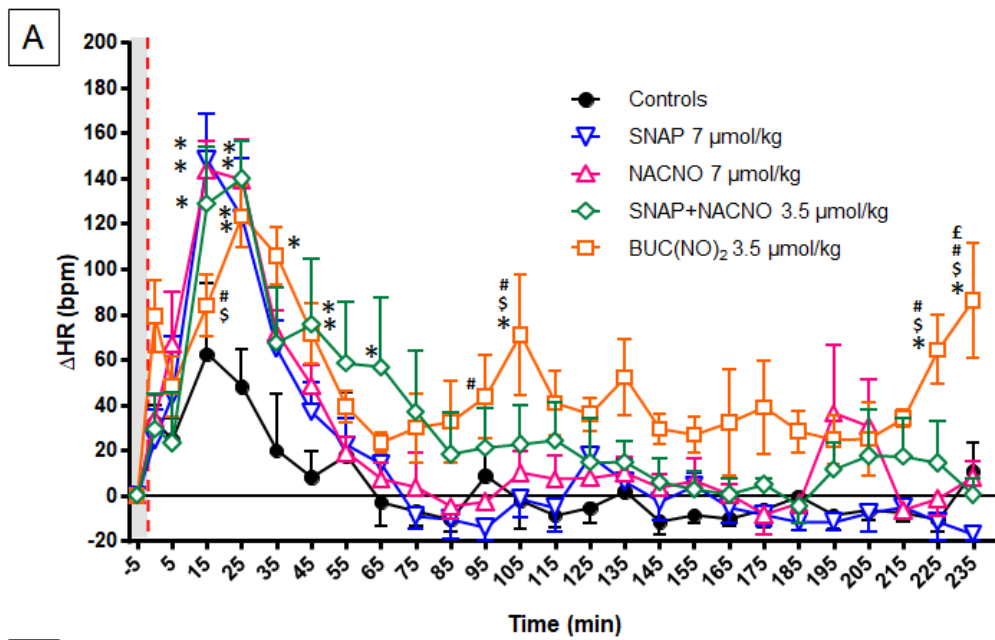


Figure 7. Impact of low (panel A), medium (panel B) and high (panel C) doses of S-nitroso-N-acetylpenicillamine (SNAP), S-nitroso-N-acetylcysteine (NACNO), the mixture SNAP+NACNO and S,S'-dinitrosobucillamine (BUC(NO)₂) on heart rate variations (Δ HR) versus baseline.

For a better clarity, only one out of two values was plotted on the graph. Doses were compared on the basis of an equivalent 'NO-load (half dose for SNAP+NACNO and BUC(NO)₂ versus mononitrosothiols). Each animal (n = 5) received all the drugs, each dose of each drug separated a by 2-day wash-out period. Grey boxes represent the duration of anesthesia and the red vertical dashed line the time of injection. *: p < 0,05 vs controls; #: p < 0,05 vs SNAP; \$: p < 0,05 vs NACNO; £: p < 0,05 vs SNAP+NACNO; Panel A: $p_{\text{interaction}} < 10^{-4}$; $p_{\text{drug}} = 0.0007$; $p_{\text{time}} < 10^{-4}$; Panel B: $p_{\text{interaction}} = 0.0853$; $p_{\text{drug}} = 0.0044$; $p_{\text{time}} < 10^{-4}$; Panel C: $p_{\text{interaction}} < 10^{-4}$; $p_{\text{drug}} = 0.0260$; $p_{\text{time}} < 10^{-4}$; (two-way ANOVA; *post-hoc* Bonferroni test).

Table 2. Maximal mean arterial pressure effects of S-nitroso-N-acetylpenicillamine (SNAP), S-nitroso-N-acetylcysteine (NACNO), SNAP+NACNO and S,S'-dinitrosobucillamine (BUC(NO)₂).

$p_{\text{interaction}} = 0.1463$, $p_{\text{dose}} = 0.0009$ and $p_{\text{drug}} = 0.0090$ (two-way ANOVA; *post-hoc* Bonferroni test).

	SNAP			NACNO			SNAP+NACNO			BUC(NO) ₂		
Dose (µmol/kg)	3.5	7	14	3.5	7	14	3.5	7	14	3.5	7	14
Δ MAP (mmHg)	-18 ±6	-28 ±6	-28 ±10	-16 ±7	-24 ±11	-46 ±6	-29 ±2	-47 ±6	-43 ±7	-36 ±5	-29 ±5	-62 ±4

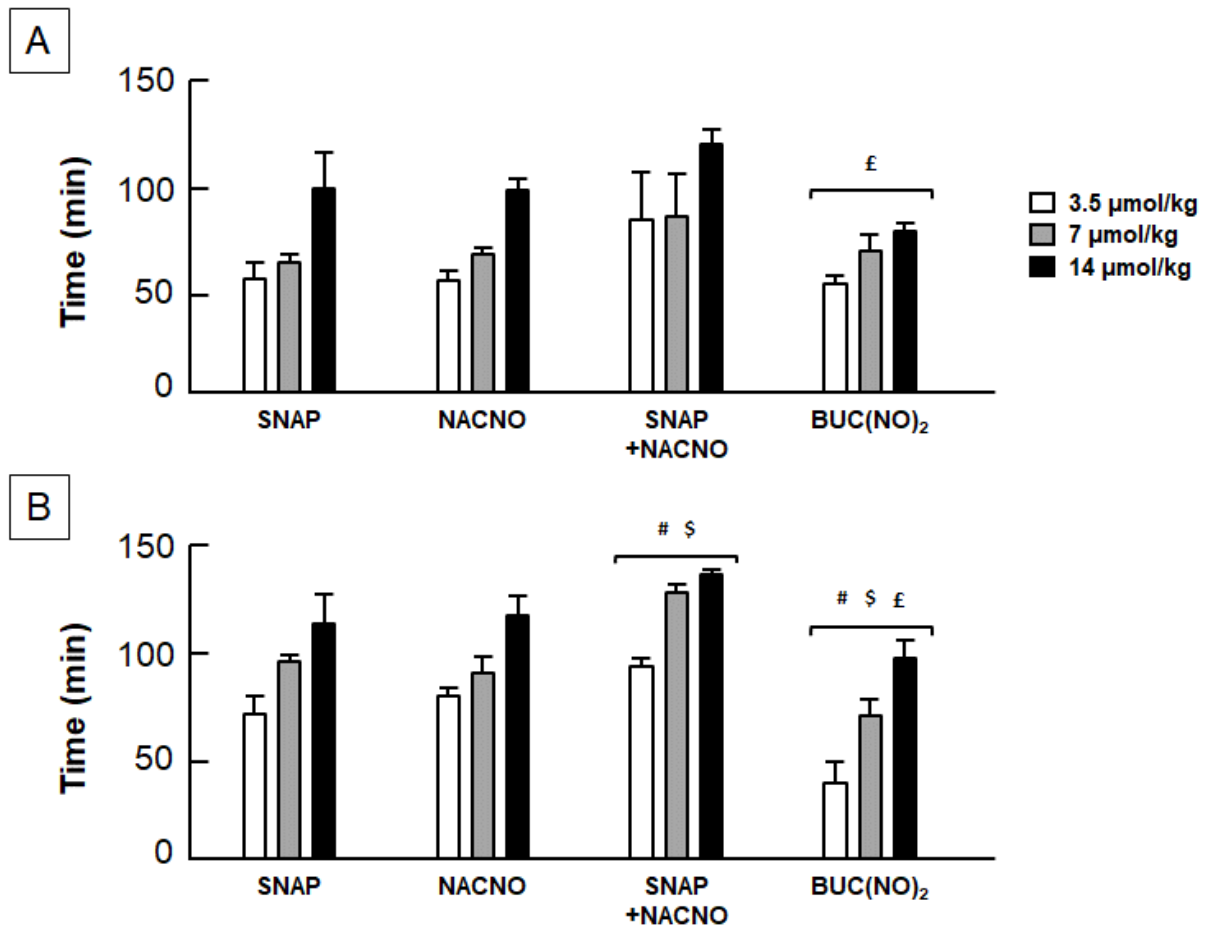


Figure 8. Duration of effect of *S*-nitroso-*N*-acetylpenicillamine (SNAP), *S*-nitroso-*N*-acetylcysteine (NACNO), the mixture SNAP + NACNO and *S,S'*-dinitrosobucillamine (BUC(NO)₂) on heart rate (HR, panel A) and pulse arterial pressure (PAP, Panel B).

#: $p < 0,05$ vs SNAP; \$: $p < 0,05$ vs NACNO; £: $p < 0,05$ vs SNAP+NACNO; Panel A: $p_{\text{interaction}} = 0.6248$; p_{drug} and $p_{\text{dose}} < 10^{-4}$; Panel B: $p_{\text{interaction}} = 0.9232$; $p_{\text{drug}} = 0.0127$; $p_{\text{dose}} < 10^{-4}$; (two-way ANOVA; *post-hoc* Bonferroni test).

4. DISCUSSION

S,S'-dinitrosobucillamine seems to induce large and fast release of [•]NO *in vivo*, as reflected by the stronger hypotension than the [•]NO-equimolar dose of SNAP+NACNO mixture (14 μmol/kg) and the shorter duration of effect on PAP compared to other RSNO. This parallels the *in vitro* results obtained in previous studies realized on isolated aortic rings, in which BUC(NO)₂ induced relaxation for the smallest concentration (Table 3, and [11]).

Table 3. Physicochemical and *ex vivo* vasorelaxant properties of *S*-nitroso-*N*-acetylpenicillamine (SNAP), *S*-nitroso-*N*-acetylcysteine (NACNO), SNAP+NACNO and *S,S'*-dinitrosobucillamine (BUC(NO)₂).

Stability (expressed as RSNO half-life) was determined in a Krebs medium at 37°C, pH 7.4. Hydrophobicity, determined by the partition coefficient (clog P), and [•]NO/RSNO mass ratio were calculated from ChemDraw software (CambridgeSoft, Perkin-Elmer, USA). The [•]NO content ([NO_x]) released from Wistar rat aortic rings exposed to RSNO was measured using the fluorogenic probe DAF-2 DA (4,5-diaminofluorescein diacetate). The vasorelaxant effects were evaluated *via* the pD₂ values (-log EC₅₀) from concentration response curves of isolated aortic rings precontracted with phenylephrine. Results are issued from [11].

	Half-life (h)	clog P	[•] NO/RSNO mass ratio	[NO _x] (μM)	pD ₂
SNAP	5	0.08	0.16	-	6.7
NACNO	63	- 0.46	0.14	-	6.4
SNAP+NACNO	-	-	0.15	420	6.7
BUC(NO) ₂	13	1.08	0.21	650	7.8

In the present study, changes in PAP were used to evaluate the duration of the RSNO effects. PAP is a function of arterial compliance/elastance, cardiac output and arterial tone, neither of which were measured in the present study as the protocols would have been too stressful for the animals. However, we used the duration of effect on PAP as a measure of the duration of the effect of RSNO, as (i) we previously published similar approach in [17; 18] and (ii) RSNO are known to induce large venodilation [26]. Venodilation decreases venous return and cardiac preload and thus decreases stroke volume, the main factor controlling PAP. Therefore, PAP would decrease. We previously showed by direct measurements of aortic pulse wave velocity [27] that [•]NO-donor administration did not change the second factor controlling PAP, *i.e.* aortic wall elasticity. We thus suggest that the fall in PAP is most likely related to a fall in stroke volume consecutive to venodilation. However, we cannot rule out that other factors are involved in the effect of RSNO on stroke volume and PAP. A direct positive myocardial effect of RSNO [28] and the improvement of cardiac function due to hypotension-induced decrease in cardiac afterload or to baroreflex-stimulated sympathetic response might both compensate the fall in stroke volume and reduce or shorten the impact of RSNO on PAP.

We did not correlate these durations with plasmatic levels of the drugs as pharmacokinetics of RSNO and/or $\cdot\text{NO}$ remain difficult to perform *in vivo*. The literature classically describes numerous pre-analytical and analytical difficulties to monitor plasma concentrations of RSNO such as *S*-nitrosoglutathione (GSNO) [29], in relationship with their poor stability (*e.g.* light, temperature and enzymes) [30]. For example, physiological concentration of GSNO is still a matter of debate, ranging from 0.00135 ± 0.00046 to $1.78 \pm 0.76 \mu\text{M}$ [29]. In their recent paper [14], Heikal *et al.* attempted to evaluate the pharmacokinetic profiles of GSNO and SNOPCs by measuring both the total RSNO content in fractionated blood (plasma *vs.* blood cells) using gas-phase chemiluminescence reaction with ozone and the total nitrate and nitrite species (NO_x) using a Griess colorimetric-based method. Despite marked differences in hemodynamic effects, they failed to see any difference in the pharmacokinetic profiles of these drugs, suggesting that blood monitoring of total RSNO and NO_x might not be sensitive enough to enable the determination of the pharmacokinetic profiles of RSNO.

In order to assess the metabolism of $\text{BUC}(\text{NO})_2$, we used an *in vitro* approach consisting in loading freshly prepared plasma with RSNO. In this biological environment, we observed a significant faster degradation of $\text{BUC}(\text{NO})_2$ compared with the other RSNO. Even though this approach cannot be considered as a pharmacokinetic study, these results are consistent with our *in silico* and *in vivo* results and seem to confirm a faster metabolism for $\text{BUC}(\text{NO})_2$.

Assuming a 100% $\cdot\text{NO}$ release, we compared, with respect to the molar concentrations of $\cdot\text{NO}$, the effects of the dinitrosothiol $\text{BUC}(\text{NO})_2$ and the SNAP+NACNO mixture, mononitrosothiols and other $\cdot\text{NO}$ -donors, *i.e.* isosorbide dinitrate (ISDN) and sodium nitroprusside (SNP) (Table 4). For a similar $\cdot\text{NO}$ -load, $\text{BUC}(\text{NO})_2$ induces the shortest effects. The duration of its effects is half of the value obtained with SNAP+NACNO mixture and it is no longer than that of mononitrosothiols such as GSNO (Table 4 and [17; 18]). When ISDN was injected subcutaneously, it did not induce any significant hypotension but a 15 mmHg decrease in PAP which lasted 37 min even at very high doses. Concerning SNP, the efficient dose to induce hypotension was $0.35 \mu\text{mol/kg}$ (0.0035 and $0.035 \mu\text{mol/kg}$ had no effect), with a -17 mmHg decrease in PAP lasting almost 100 min. At the dose of $3.5 \mu\text{mol/kg}$, 2 out of the 5 rats died while the remaining ones underwent severe and prolonged hypotension (which led us to sacrifice the rats for exceeding the ethical limit points). These data led to several assumptions.

Table 4. Decreases in mean and pulse arterial pressures and duration of effects of *S*-nitroso-*N*-acetylpenicillamine (SNAP), *S*-nitroso-*N*-acetylcysteine (NACNO), SNAP+NACNO, *S,S'*-dinitrosobucillamine (BUC(NO)₂), *S*-nitrosogluthathione (GSNO), isosorbide dinitrate (ISDN) and sodium nitroprusside (SNP) at different doses and 'NO - loads (subcutaneous administration).

Molecule	Dose (μmol/kg)	'NO-load (μmol/kg)	ΔMAP (mmHg)	Duration PAP (min)	Reference
SNAP	7.0	7	-28	95	Present results
NACNO	7.0	7	-24	89	
SNAP+NACNO	3.5	7	-29	92	
BUC(NO) ₂	3.5	7	-36	37	
SNAP	17.0	17	-27	65	[17]
SNAP	14.0	14	-28	113	Present results
NACNO	14.0	14	-46	117	
SNAP+NACNO	7.0	14	-47	128	
BUC(NO) ₂	7.0	14	-29	69	
GSNO	11.0	11	-24	60	[18]
SNAP	34.0	34	-30	85	[17]
SNAP+NACNO	14.0	28	-43	136	Present results
BUC(NO) ₂	14.0	28	-62	96	
GSNO	22.0	22	-37	65	[18]
ISDN	21.0 (42.0, 85.0)	42 (84, 170)	No effect	37	Present results
SNP	0.035	0.035	No effect	No effect	
SNP	0.35	0.35	-49	96	

First, all RSNO produce *in vivo* both arterial (effect on MAP) and venous (effect on PAP) dilations. Despite the lack of report on PAP data, this can be assumed even for SNOPCs, with regards to the raw blood pressure recordings provided by Heikal *et al.* [14]. This is also the case for SNP but not for ISDN, which only produces a decrease in PAP, reflecting venodilation.

Second, regarding the arterial effect, RSNO seem less efficient than SNP, as they require a 20 to 40-fold higher 'NO-load to produce similar hypotension. However, they appear safer, with a larger margin of safety, as they do not release cyanate leading to toxicity and death as observed at the end of this study (injection of SNP). The protocol used by Heikal *et al.* did not allow us to compare the arterial effect of SNOPCs to that of the drugs used in the present report as 1) the different routes of administration used (subcutaneous *vs.* intravenous) obviously imply a different dose range and 2) hemodynamics were not recorded in the same conditions (awake rats *vs.* anesthetized mice).

Third, regarding the venous effect (the main effect of ISDN and other organic nitrates explaining their use in angina pectoris, for instance, as venodilation decreases cardiac preload), RSNO seem more efficient than ISDN as they produce, for a much lower $\cdot\text{NO}$ -load, a comparable effect (-15 mmHg in PAP) which lasts longer. For example, $\text{BUC}(\text{NO})_2$ induces the same effect duration on PAP (37 min) than ISDN but with a 6-fold lower $\cdot\text{NO}$ -load.

Finally, more than the total amount of administered $\cdot\text{NO}$, the nature of the carrier and the number of SNO moieties seem to be major determinants of the biological activities of RSNO. At high doses, $\text{BUC}(\text{NO})_2$ produced the most pronounced decrease in MAP (-62 mmHg), an effect that tend to be superior to that of the SNAP+NACNO mixture exhibiting the same $\cdot\text{NO}$ -load (Figure 6 and Tables 2 and 4). This differential effect at high doses seems to be rather the consequence of a plateau effect reached at the medium dose for SNAP+NACNO, as the highest dose did not produce any further reduction in MAP. This does not seem to be the case for $\text{BUC}(\text{NO})_2$ as the highest dose induced a twofold higher impact on MAP variation compared with the medium dose. This is probably related to the faster metabolism of $\text{BUC}(\text{NO})_2$ as suggested by our *in silico* findings and confirmed by our new data obtained in plasma. As the release of the first $\cdot\text{NO}$ moiety facilitates the release of the second one (see below), this likely contributes to reach higher levels of $\cdot\text{NO}$ than with the SNAP+NACNO mixture. Similar results were obtained by Heikal *et al.* when they administered SNOPCs and GSNO *in vivo* at equal molar concentrations of SNO. The SNOPC carrying 6 SNO moieties induced a more pronounced decrease in blood pressure than GSNO or the SNOPC carrying 2 SNO [14]. Taken together, these data suggest that the intrinsic molecular characteristics of the SNO-carrier are a key determinant of the RSNO biological activity. In the present work, we have studied the $\cdot\text{NO}$ dissociation mechanism in $\text{BUC}(\text{NO})_2$ and compared the results to those previously obtained for SNAP and NACNO [20]. As discussed before, the homolytic dissociation in SNAP and NACNO can be assumed to be a barrierless process. The calculated reaction free energies for $\cdot\text{NO}$ dissociation in SNAP and NACNO were 12.8 and 17.8 kcal.mol⁻¹, respectively [20]. For $\text{BUC}(\text{NO})_2$, all dissociation processes lie within the range of 16-17 kcal.mol⁻¹, which suggests that dissociation in $\text{BUC}(\text{NO})_2$ is significantly less favorable than in SNAP and slightly more favorable than in NACNO. However, $\text{BUC}(\text{NO})_2$ induced the shortest *in vivo* observed effects (Table 4).

Several explanations could contribute to this discrepancy. First, given the adopted assumptions in our calculations, these kinetic constant values are only approximations to the real experimental values. Moreover, the *in silico* theoretical results cannot augur for a potential faster degradation rate for $\text{BUC}(\text{NO})_2$ than for NACNO and SNAP *in vivo*. Indeed,

we previously showed *in vitro* that the denitrosation pathway [12; 31] of BUC(NO)₂ depends on the protein disulfide isomerase (PDI) activity, which is not the case for either NACNO or SNAP [11]. While this remains to be evaluated *in vivo*, this could explain why BUC(NO)₂ has a shorter effect compared to mononitrosothiols and the mixture. In their studies, Heikal *et al.* also tried to explain the differences of [•]NO release from RSNO studying the effect of various enzymes [12]. While PDI has an effect on both GSNO and SNOPCs, γ -glutamyl transpeptidase only had an effect on GSNO. Taken together, these results highlight the importance of enzyme-dependent metabolism in the observed difference of RSNO action.

Finally, the faster [•]NO release from BUC(NO)₂ could also rely on specific physicochemical properties such as the molecular electronic structure of BUC(NO)₂. After the release of the first [•]NO moiety (possibly related to enzymatic processes, as suggested above), the resulting sulfur free radical reacts with the remaining SNO group leading to the immediate release of the second [•]NO moiety and formation of an intramolecular disulfide bond (Figure 1). This was confirmed by the LC-MS/MS analysis of the degradation products of BUC(NO)₂ under two operating conditions (heating and exposure to an oxidizing agent *i.e.* H₂O₂) showing the presence of a degradation product including an intramolecular disulfide bond (Figure 2). A similar hypothesis has been proposed for SNOPCs, as they are prone to a more rapid physicochemical degradation *in vitro* than GSNO, which correlates with the formation of intramolecular disulfide bonds, assessed by mass spectrometry [32]. This fast release of the first [•]NO moiety followed by the formation of an intramolecular disulfide bridge can contribute to the faster metabolism of BUC(NO)₂ observed *in vitro* in plasma and thus to the its shorter effect compared to NACNO and SNAP. The more lipophilic nature of BUC(NO)₂ compared to SNAP and NACNO (Table 3, [11]) could also contribute to the faster [•]NO release. When administered subcutaneously, the lipophilic properties of BUC(NO)₂ may accelerate its flow through cellular membranes within blood vessels and thus lead to a faster systemic effect.

In the field of RSNO and their clinical use, the most important challenge actually is to control kinetics and amounts of [•]NO to be released, especially during pathologies where oxidative stress may lead to nitrosative derivation of [•]NO when released from RSNO [33]. In this context, the capacity of BUC(NO)₂ to quickly release a great quantity of [•]NO may be considered as a disadvantage. However, when compared to other commercially available fast [•]NO donors such as SNP, BUC(NO)₂ would certainly not induce side effects, as bucillamine, when used as an anti-inflammatory and antioxidant agent, does not produce serious adverse events [16]. Furthermore, as lipophilic molecules are easier to encapsulate [34], formulation

542 of BUC(NO)₂ would be a good strategy to increase duration of its effects in pathologies that
543 requires a slow and sustained release of [•]NO (*e.g.* post-stroke, [17]).

544 As a conclusion, the hypothesis that increasing [•]NO payload on polythiols would
545 increase the efficiency of corresponding RSNO seems to depend on the nature of the thiolated
546 molecule carrying [•]NO. Rather than increasing the number of [•]NO, attention must be paid to
547 the choice of the molecule carrying [•]NO, as numerous factors are involved in the degradation
548 of RSNO.

549 **ACKNOWLEDGMENTS**

550 **FUNDING SOURCES**

551 This work was supported by the French Ministry of Research and Education (Paris, France).

552 **DISCLOSURES**

553 None

554 REFERENCES

- 555 [1] S. Moncada, E.A. Higgs, Endogenous nitric oxide: physiology, pathology and clinical
556 relevance, *Eur. J. Clin. Invest.* 21 (1991) 361-74.
- 557 [2] J.A. Bauer, H.L. Fung, Differential hemodynamic effects and tolerance properties of
558 nitroglycerin and an S-nitrosothiol in experimental heart failure, *J. Pharmacol. Exp. Ther.* 256
559 (1991) 249-54.
- 560 [3] J.D. Parker, T. Gori, Tolerance to the organic nitrates: new ideas, new mechanisms,
561 continued mystery, *Circulation* 104 (2001) 2263-5.
- 562 [4] U. Förstermann, T. Münzel, Endothelial nitric oxide synthase in vascular disease: from
563 marvel to menace, *Circulation* 113 (2006) 1708-14.
- 564 [5] C. Gaucher, A. Boudier, F. Dahboul, M. Parent, P. Leroy, S-nitrosation/denitrosation in
565 cardiovascular pathologies: facts and concepts for the rational design of S-nitrosothiols, *Curr.*
566 *Pharm. Des.* 19 (2013) 458-72.
- 567 [6] C. Mancuso, A. Bonsignore, E. Di Stasio, A. Mordente, R. Motterlini, Bilirubin and S-
568 nitrosothiols interaction: evidence for a possible role of bilirubin as a scavenger of nitric
569 oxide, *Biochem. Pharmacol.* 66 (2003) 2355-63.
- 570 [7] J.L. Alencar, I. Lobysheva, K. Chalupsky, M. Geffard, F. Nepveu, J.C. Stoclet, B. Muller,
571 S-nitrosating nitric oxide donors induce long-lasting inhibition of contraction in isolated
572 arteries, *J. Pharmacol. Exp. Ther.* 307 (2003) 152-9.
- 573 [8] B. Furlong, A.H. Henderson, M.J. Lewis, J.A. Smith, Endothelium-derived relaxing factor
574 inhibits in vitro platelet aggregation, *Br. J. Pharmacol.* 90 (1987) 687-92.
- 575 [9] H. Al-Sa'doni, A. Ferro, S-nitrosothiols as nitric oxide-donors: chemistry, biology and
576 possible future therapeutic applications, *Curr. Med. Chem.* 11 (2004) 2679-90.
- 577 [10] W. Wu, C. Perrin-Sarrado, H. Ming, I. Lartaud, P. Maincent, X.M. Hu, A. Sapin-Minet,
578 C. Gaucher, Polymer nanocomposites enhance S-nitrosoglutathione intestinal absorption and
579 promote the formation of releasable nitric oxide stores in rat aorta, *Nanomed. Nanotechnol.*
580 *Biol. Med.* 12 (2016) 1795-1803.
- 581 [11] F. Dahboul, C. Perrin-Sarrado, A. Boudier, I. Lartaud, R. Schneider, P. Leroy, S,S'-
582 dinitrosobucillamine, a new nitric oxide donor, induces a better vasorelaxation than other S-
583 nitrosothiols, *Eur. J. Pharmacol.* 730 (2014) 171-9.
- 584 [12] L. Heikal, P.I. Aaronson, A. Ferro, M. Nandi, G.P. Martin, L.A. Dailey, S-
585 nitrosophytochelates: investigation of the bioactivity of an oligopeptide nitric oxide delivery
586 system, *Biomacromolecules* 12 (2011) 2103-13.
- 587 [13] I.L. Megson, I.R. Greig, A.R. Butler, G.A. Gray, D.J. Webb, Therapeutic potential of S-
588 nitrosothiols as nitric oxide donor drugs, *Scott. Med. J.* 42 (1997) 88-9.
- 589 [14] L. Heikal, A. Starr, G.P. Martin, M. Nandi, L.A. Dailey, In vivo pharmacological activity
590 and biodistribution of S-nitrosophytochelates after intravenous and intranasal administration
591 in mice, *Nitric Oxide* 59 (2016) 1-9.
- 592 [15] L.D. Horwitz, Bucillamine: a potent thiol donor with multiple clinical applications,
593 *Cardiovasc. Drug Rev.* 21 (2003) 77-90.
- 594 [16] N. Sekiguchi, H. Kameda, K. Amano, T. Takeuchi, Efficacy and safety of bucillamine, a
595 D-penicillamine analogue, in patients with active rheumatoid arthritis, *Mod. Rheumatol.* 16
596 (2006) 85-91.

597 [17] M. Parent, A. Boudier, F. Dupuis, C. Nouvel, A. Sapin, I. Lartaud, J.L. Six, P. Leroy, P.
598 Maincent, Are in situ formulations the keys for the therapeutic future of S-nitrosothiols?, Eur.
599 J. Pharm. Biopharm. 85 (2013) 640-649.

600 [18] M. Parent, A. Boudier, J. Perrin, C. Vigneron, P. Maincent, N. Violle, J.F. Bisson, I.
601 Lartaud, F. Dupuis, In Situ Microparticles Loaded with S-Nitrosoglutathione Protect from
602 Stroke, PLoS One 10 (2015) e0144659.

603 [19] M. Parent, F. Dahboul, R. Schneider, I. Clarot, P. Maincent, P. Leroy, A. Boudier, A
604 complete physicochemical identity card of S-nitrosoglutathione, Curr. Pharm. Anal. 9 (2013)
605 31-42.

606 [20] B. Meyer, A. Genoni, A. Boudier, P. Leroy, M.F. Ruiz-Lopez, Structure and Stability
607 Studies of Pharmacologically Relevant S-Nitrosothiols: A Theoretical Approach, J. Phys.
608 Chem. A 120 (2016) 4191-200.

609 [21] J.P. Perdew, Y. Wang, Accurate and simple analytic representation of the electron-gas
610 correlation energy, Phys Rev B Condens Matter 45 (1992) 13244-13249.

611 [22] E. Cancès, B. Mennucci, J. Tomasi, A new integral equation formalism for the
612 polarizable continuum model: Theoretical background and applications to isotropic and
613 anisotropic dielectrics., J. Chem. Phys. 107 (1997) 3032-3041.

614 [23] M.J. Frisch, G.W. Trucks, H.B. Schlegel, G.E. Scuseria, M.A. Robb, J.R. Cheeseman, G.
615 Scalmani, V. Barone, B. Mennucci, G.A. Petersson, H. Nakatsuji, M. Caricato, X. Li, H.P.
616 Hratchian, A.F. Izmaylov, J. Bloino, G. Zheng, J.L. Sonnenberg, M. Hada, M. Ehara, K.
617 Toyota, R. Fukuda, J. Hasegawa, M. Ishida, T. Nakajima, Y. Honda, O. Kitao, H. Nakai, T.
618 Vreven, J.A. Montgomery Jr., J.E. Peralta, F. Ogliaro, M.J. Bearpark, J. Heyd, E.N. Brothers,
619 K.N. Kudin, V.N. Staroverov, R. Kobayashi, J. Normand, K. Raghavachari, A.P. Rendell, J.C.
620 Burant, S.S. Iyengar, J. Tomasi, M. Cossi, N. Rega, N.J. Millam, M. Klene, J.E. Knox, J.B.
621 Cross, V. Bakken, C. Adamo, J. Jaramillo, R. Gomperts, R.E. Stratmann, O. Yazyev, A.J.
622 Austin, R. Cammi, C. Pomelli, J.W. Ochterski, R.L. Martin, K. Morokuma, V.G. Zakrzewski,
623 G.A. Voth, P. Salvador, J.J. Dannenberg, S. Dapprich, A.D. Daniels, Ö. Farkas, J.B.
624 Foresman, J.V. Ortiz, J. Cioslowski, D.J. Fox, Gaussian 09, Gaussian, Inc., Wallingford, CT,
625 USA, 2009.

626 [24] P. Pikul, M. Jamrogiewicz, J. Nowakowska, W. Hewelt-Belka, K. Ciura, Forced
627 Degradation Studies of Ivabradine and In Silico Toxicology Predictions for Its New
628 Designated Impurities, Front. Pharmacol. 7 (2016) 117.

629 [25] J. Sun, X. Zhang, M. Broderick, H. Fein, Measurement of Nitric Oxide Production in
630 Biological Systems by Using Griess Reaction Assay, Sensors 3 (2003) 276-284.

631 [26] N. Sogo, C. Campanella, D.J. Webb, I.L. Megson, S-nitrosothiols cause prolonged, nitric
632 oxide-mediated relaxation in human saphenous vein and internal mammary artery: therapeutic
633 potential in bypass surgery, Br. J. Pharmacol. 131 (2000) 1236-44.

634 [27] N. Niederhoffer, V. Marque, I. Lartaud-Idjouadiene, C. Duvivier, R. Peslin, J. Atkinson,
635 Vasodilators, aortic elasticity, and ventricular end-systolic stress in nonanesthetized
636 unrestrained rats, Hypertension 30 (1997) 1169-74.

637 [28] T. Rassaf, L.W. Poll, P. Brouzos, T. Lauer, M. Totzeck, P. Kleinbongard, P. Gharini, K.
638 Andersen, R. Schulz, G. Heusch, U. Modder, M. Kelm, Positive effects of nitric oxide on left
639 ventricular function in humans, Eur. Heart J. 27 (2006) 1699-705.

640 [29] D. Giustarini, A. Milzani, I. Dalle-Donne, R. Rossi, Detection of S-nitrosothiols in
641 biological fluids: a comparison among the most widely applied methodologies, *J. Chromatogr.*
642 *B* 851 (2007) 124-139.

643 [30] E. Bramanti, V. Angeli, Z. Mester, A. Pompella, A. Paolicchi, A. D'Ulivo, Determination
644 of S-nitrosoglutathione in plasma: comparison of two methods, *Talanta* 81 (2010) 1295-9.

645 [31] R. Xiao, J. Lundström-Ljung, A. Holmgren, H.F. Gilbert, Catalysis of thiol/disulfide
646 exchange. Glutaredoxin 1 and protein-disulfide isomerase use different mechanisms to
647 enhance oxidase and reductase activities, *J. Biol. Chem.* 280 (2005) 21099-106.

648 [32] L. Heikal, G.P. Martin, L.A. Dailey, Characterisation of the decomposition behaviour of
649 S-nitrosoglutathione and a new class of analogues: S-Nitrosophytochelatin, *Nitric Oxide* 20
650 (2009) 157-65.

651 [33] Y. Liu, C. Xia, R. Wang, J. Zhang, T. Yin, Y. Ma, L. Tao, The opposite effects of nitric
652 oxide donor, S-nitrosoglutathione, on myocardial ischemia/reperfusion injury in diabetic and
653 non-diabetic mice, *Clin. Exp. Pharmacol. Physiol.* (2017).

654 [34] M. Parent, C. Nouvel, M. Koerber, A. Sapin, P. Maincent, A. Boudier, PLGA in situ
655 implants formed by phase inversion: critical physicochemical parameters to modulate drug
656 release, *J. Control. Release* 172 (2013) 292-304.

657